Electronic Supplementary Material (ESI) for Lab on a Chip.

Supporting Information

On-chip Sample Preparation and Analyte Quantification using a Microfluidic Aqueous Two Phase Extraction coupled to an Immunoassay

Ruben R. G. Soares [a, c] ; Pedro Novo [a]; Ana M. Azevedo [b, c]; Pedro Fernandes [b, c]; M. Raquel Aires-Barros [b, c]; Virginia Chu [a]; João P. Conde [a, b] *

[a] INESC Microsistemas e Nanotecnologias and IN-Institute of Nanoscience and Nanotechnology, Lisbon, Portugal

[b] Department of Bioengineering, Instituto Superior Técnico, Universidade de Lisboa, Lisbon, Portugal

[c] IBB – Institute for Biotechnology and Bioengineering, Centre for Biological and Chemical Engineering, Instituto Superior Técnico, Universidade de Lisboa, Lisbon, Portugal

*Contacting Author e-mail adress: joao.conde@tecnico.ulisboa.pt

Table of Contents

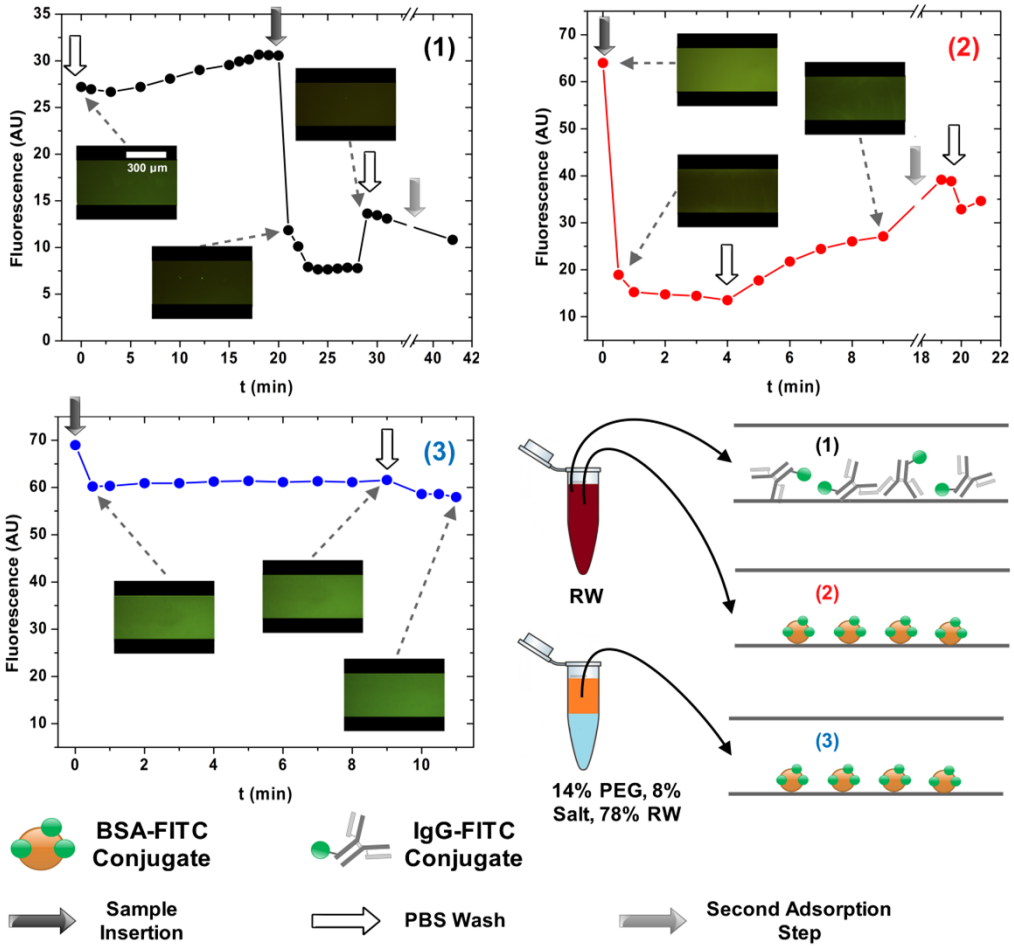

Figure S1 Fluorescence quenching experiments performed for adsorbed anti-mouse IgG-FITC (figure (1)) or BSA-FITC (figures (2) and (3)). The breaks in the x axis correspond to 10 min of a second adsorption step performed away from the microscope. The adsorption steps were performed by flowing 50 µg/mL IgG-FITC (figure (1)) or BSA-FITC (figures (2) and (3)) solutions prepared in PBS at 0.5 µL/min for 10 min. Red wine (figures (1) and (2)) or PRP samples (figure 3)) were inserted at a flow rate of 0.5 µL/min while washing steps with PBS were performed at 5 µL/min. All figures have the same size scale shown in (1). The results show that for both BSA-FITC and IgG-FITC coated channels, the fluorescence drops almost instantly to about 25% of the initial value when red wine (adjusted at pH 6) is flowed through the channel. Then, the intensity remains stable for several minutes. Upon washing with PBS, fluorescence is recovered to about

50% of the initial value. Finally, to confirm that the decrease of fluorescence is not due to molecular desorption, a new adsorption step with fresh BSA-FITC or IgG-FITC solutions is performed on each channel. It was observed that the fluorescence was not significantly increased after this step for neither of the channels. It can also be concluded that when a PP rich PRP was flowed into the channels instead of red wine, no significant drop in fluorescence was observed for as long as 10 min.

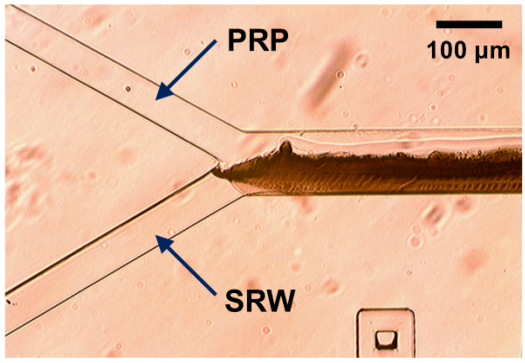

Figure S2 Highlight on the PP precipitation effect observed at the SRP-PRP interface.

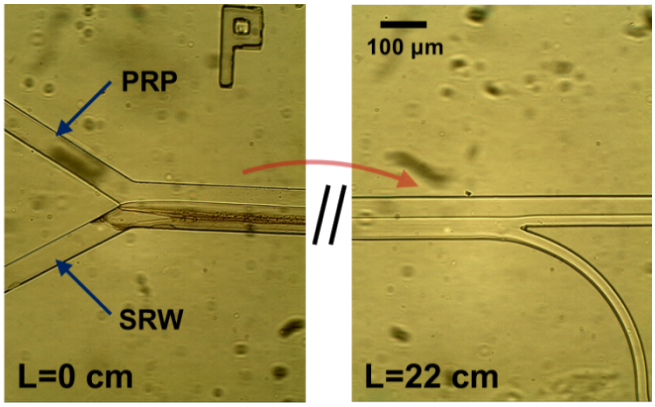

Figure S3 Microfluidic ATPE using a SRW prepared with 13.1% NaH_2PO_4/K_2HPO_4 (pH 7) and a PRP extracted from an ATPS prepared in a microtube for a total of 14% PEG 8,000 and 8% NaH_2PO_4/K_2HPO_4 (pH 7).

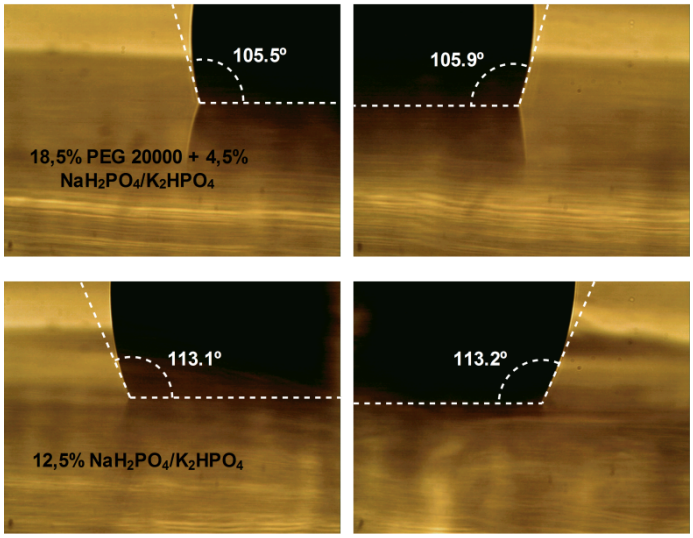

Figure S4 Contact angle measurements at the interface of each PRP and SRP with a PDMS membrane. The images were acquired with a Model #MD600 inverted microscope from AmScope, using a 10x objective. The total volume of the drop is 2.5 µL. It should be noted that more similar the hydrophobicity between the PDMS and the phase solution, the lower will be the internal angle.

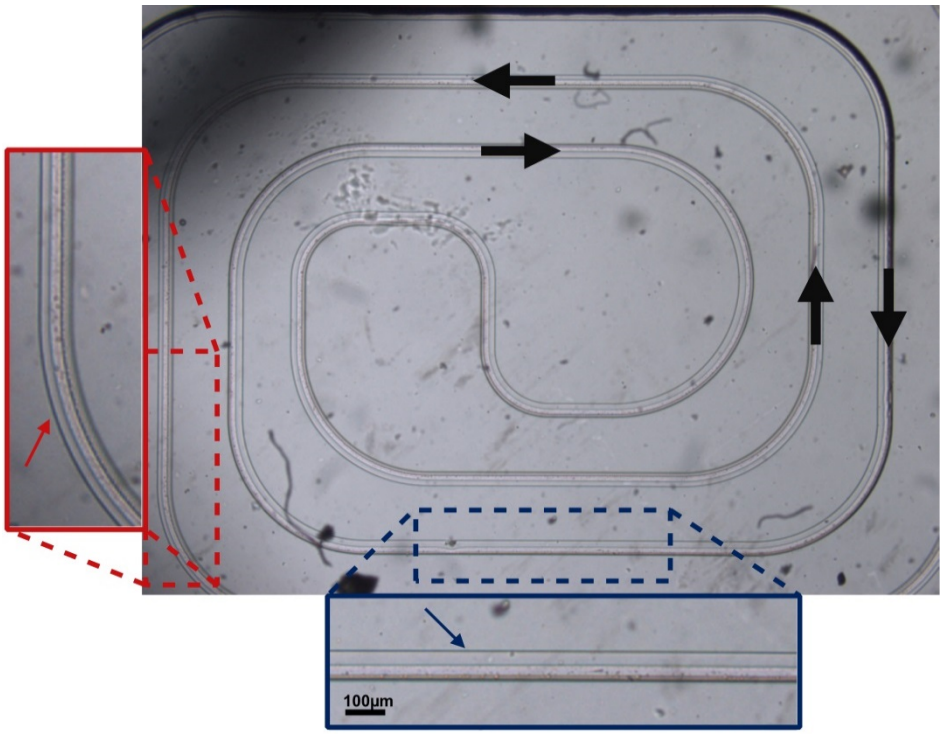

Figure S5 Bright field microscopy image of the separation channel, highlighting the decrease of the primary PRP width (identified by the arrows) with increasing *L* of the channel. The bottom highlighted section is at *L*=1.53 cm, while the left section is at *L*=4.27 cm, showing a decrease on PRP width from ≈42 µm to ≈27 µm respectively.

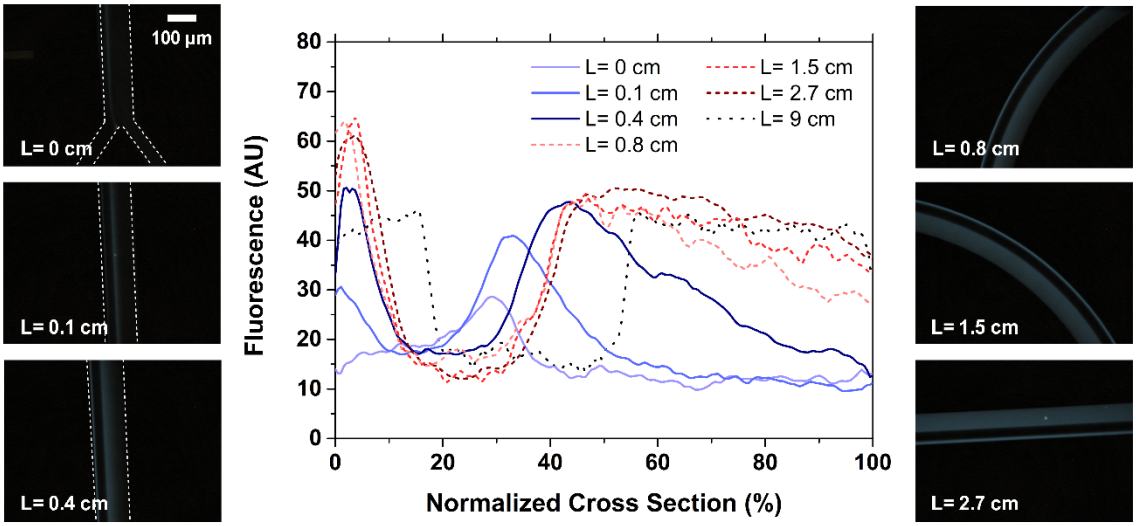

Figure S6 Cross-section OTA fluorescence emission plots at increasing *L* values, in conditions where OTA is spiked in a solution containing 12.5% NaH_2PO_4/K_2HPO_4 (pH 7) and converged with a PRP prepared with 18.5% PEG 20,000 and 4.5% NaH_2PO_4/K_2HPO_4 (pH 7).

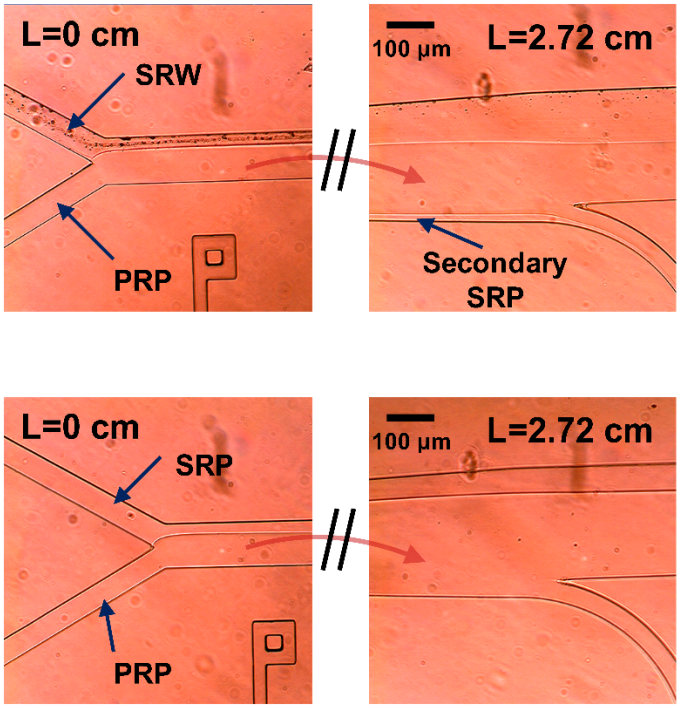

Figure S7 Microfluidic ATPE using a SRW (top) or SRP (bottom) both prepared with 12.5% NaH_2PO_4/K_2HPO_4 (pH 7) and a PRP prepared with 18.5% PEG 20,000 and 4.5% NaH_2PO_4/K_2HPO_4 (pH 7). The solutions are flowing from left to right after first adsorbing BSA on the surface of the channel by flowing a 4% (m/v) BSA solution in PBS for 5 min through both inlets and main separation channel. The formation of a secondary SRP is observed for salt spiked red and white wines but such does not occur when salt spiked MilliQ water is used.

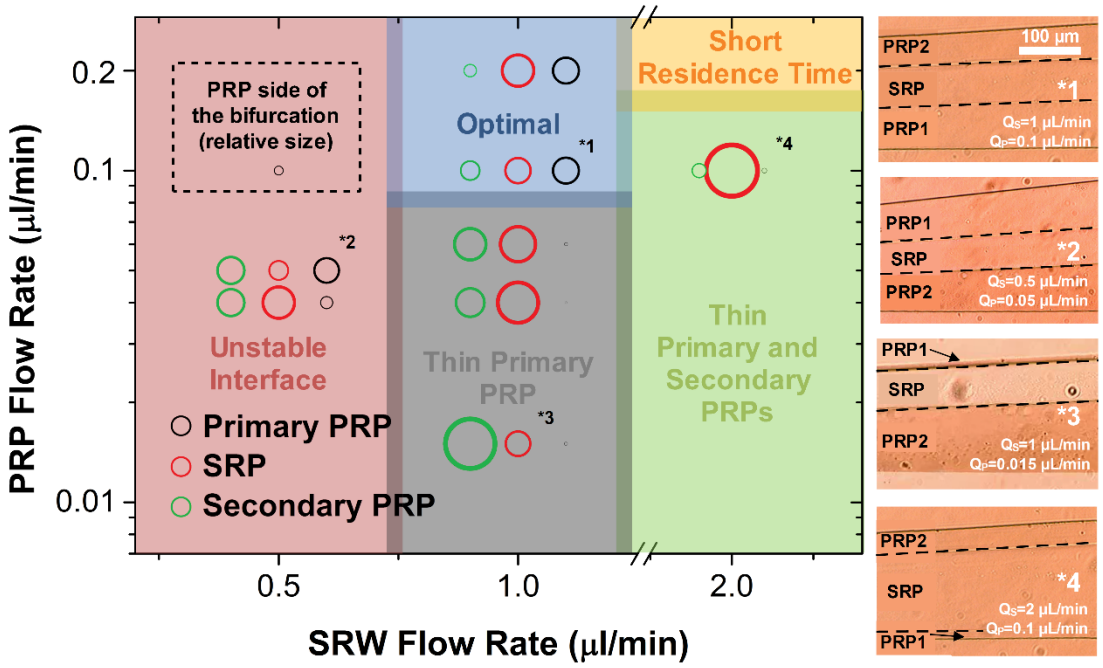

Figure S8 Bubble chart describing the main effects of the PRP and SRP flow rates on the behavior of each phase across the separation channel (L = 9 cm). The relative size of the bubbles at each pair of flow rate conditions relates to the relative size that each of the phases occupies at the channel cross-section. The black colored bubble highlighted inside the top-left dashed rectangle relates to the relative size of the collection channel whose purpose is to collect the primary PRP without contamination from the SRP. Hence, to prevent contamination, the primary PRP bubble for a given condition needs to be at least as large as the above mentioned black bubble. Each of the differently shaded regions are described as follows: **Unstable Interface-** The interface between all three phases was observed to have an unstable behavior, rendering the collection of the primary PRP impossible without sporadic contamination from the SRP; **Thin Primary PRP-** The relative volume occupied by the primary PRP was observed to be very small, rendering its collection impossible without contamination from SRP; **Thin Primary and Secondary PRPs-** The high flow rate of the SRP relative to the PRP results in a very small relative volume occupied by the primary and secondary PRPs; **Short Residence**

Time- Range not tested. However, further increasing the PRP flow rate to compensate this effect would possibly result in similar Q_R values as for the optimal region, at the cost of requiring a longer channel to keep the residence time constant. **Optimal-** Optimal set of conditions to avoid contamination. Values of Q_S = 1 µL/min and Q_P = 0.2 µL/min were selected to guarantee the absence of SRP contamination. For all of the bright field microscopy images on the right side of the figure, the liquid flow direction is from left to right. PRP1 and PRP2 refer to the primary and secondary PRPs respectively. The black dashed lines highlight the interface position.

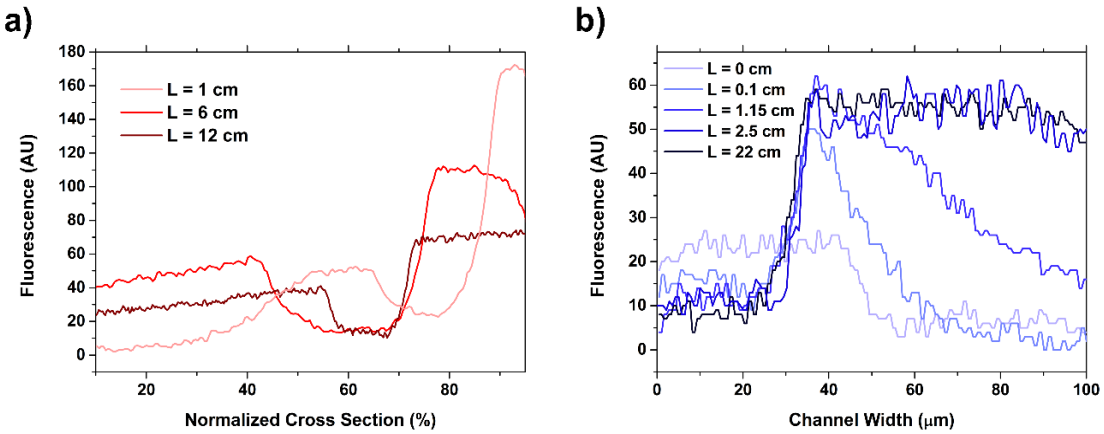

Figure S9 Cross-section fluorescence emission plots for the PP (a) and OTA (b) partition experiments presented in Figure 4, at increasing *L* values. The normalization of the cross section in (a) is in respect to the channel width. In (b), the apparent OTA concentration effect was not due to an enhanced fluorescence of OTA in the PRP originated from solvatochromic effects. This was confirmed by spiking 1 µg/mL of OTA in each of the SRP and PRP in separate microtubes, and then measuring the fluorescence emission of these solutions in a Varian (Palo Alto, CA, USA) Eclipse spectrofluorimeter (excitation and emission wavelengths set at 333 and 446 nm respectively). The obtained values were 85.16 AU for the PRP and 96.6 AU for the SRP. This result validates the concentration

effect, as the fluorescence intensities are within a 15% difference range, while the increase in fluorescence observed under the microscope was nearly 200%.

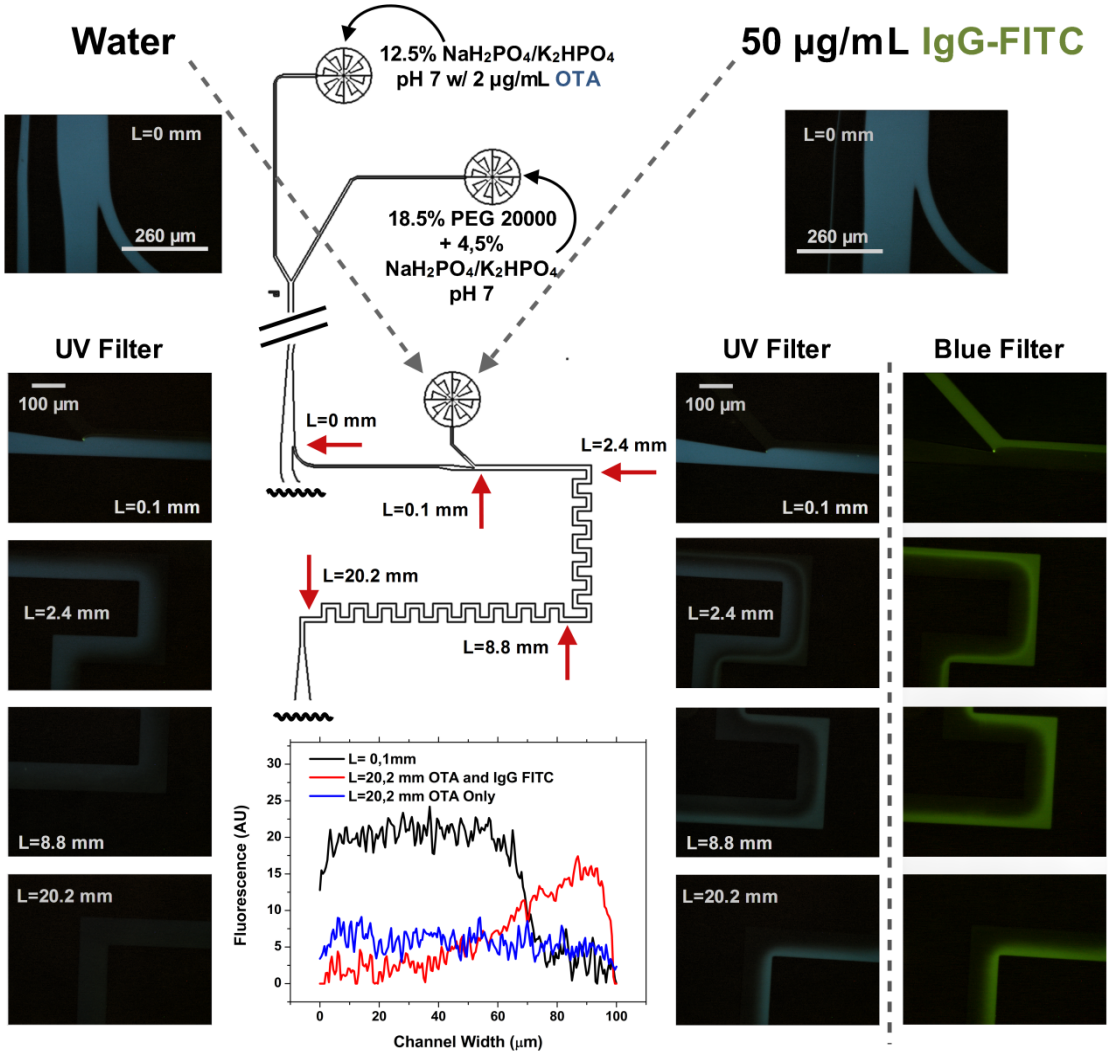

Figure S10 OTA diffusion experiments performed by converging an OTA concentrated PRP solution with water or a 50 µg/mL anti-mouse IgG-FITC solution, prepared in water. All images were acquired with an exposure time of 1 s and a gain of 3x. The side-by-side UV and blue filter images on the right were acquired with an interval of 5-10 s. All images were contrast enhanced for better visualization. The flow rates used were 1 µL/min for the SRP, 0.2 µL/min for the PRP and 0.25 µL/min for water or IgG-FITC solution. The channel cross-section fluorescence emission plot is normalized in respect to the

background. These were plotted using Image J software and relate to the UV filter acquired images. The fluorescence emission plots using both the UV and blue filters, in the presence of 50 µg/mL IgG-FITC, can be seen in Figure S11.

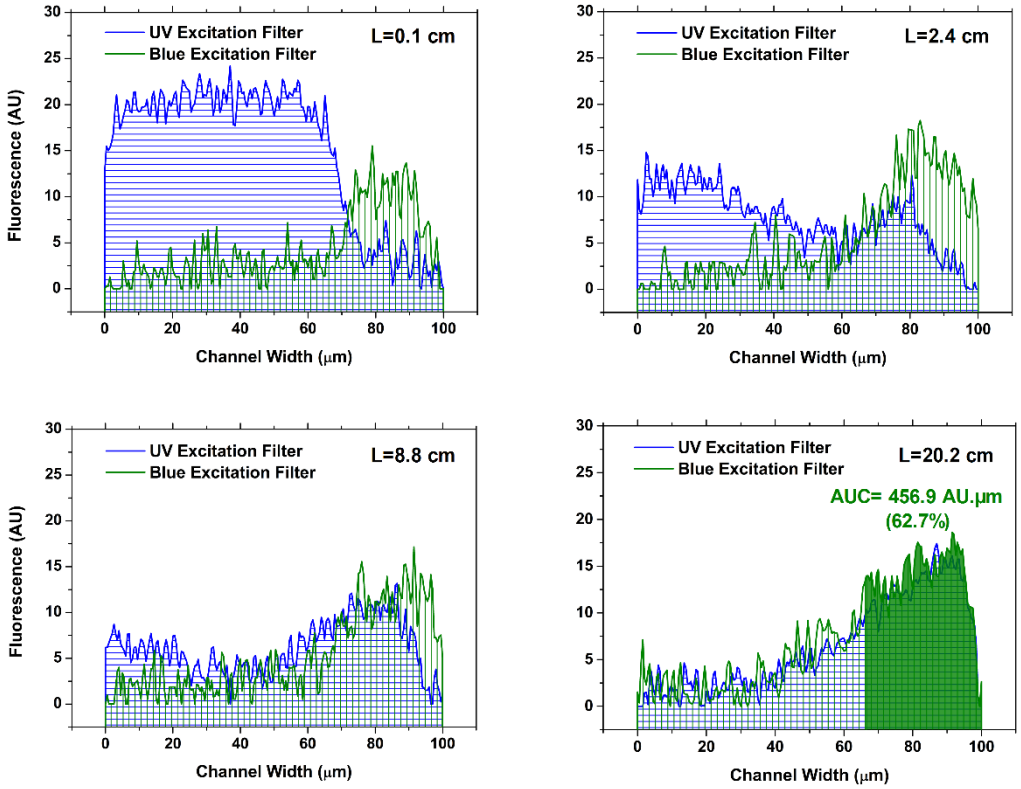

Figure S11 Channel cross section fluorescence intensity profiles, measured using ImageJ software, for the images acquired in the presence of 50 µg/mL IgG-FITC (Figure S10-right). The fluorescence emission values are normalized in respect to the background. For L=20.2, the green highlighted area corresponds to the fraction of channel redirected towards the immunoassay section downstream.

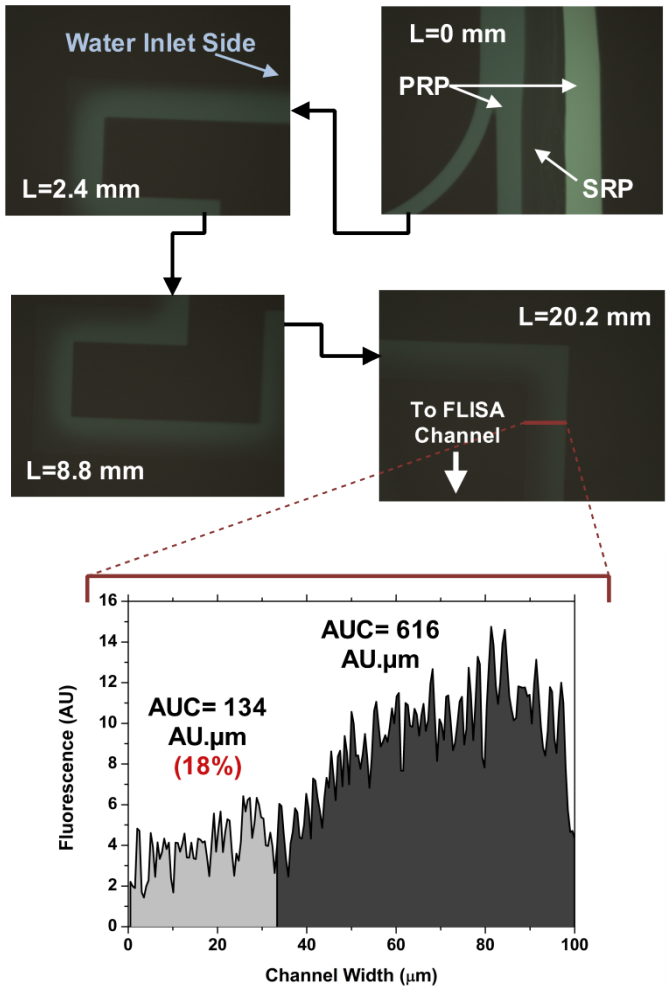

Figure S12 UV excitation filter microscopy images acquired at increasing L along the micromixer. A PRP (18.5% PEG 20,000, 4.5% NaH_2PO_4/K_2HPO_4 pH 7) and SRW (12,5% NaH_2PO_4/K_2HPO_4 pH 7 in red wine) solutions were converged downstream of *L*=0 mm, while water was being flowed into the third inlet. The areas under the curve (AUC) were integrated for each of the differently shaded regions, in which the light grey shade corresponds to the theoretical collected region (1/3 of the channel cross-section), which flows to the IC upstream.

Details on microfluidic structure operation to perform an integrated ATPE and FLISA. The sealing of the inlets/outlets was performed with 20 *ga* closed metallic adapters. The closed adapters were inserted down to about a millimeter away from the bottom PDMS membrane and are used as valves to prevent liquids from flowing into certain regions of the structure (Figure S13). A solution of OTA-BSA prepared in PBS was introduced into the icFLISA channels (ICs), highlighted in blue in Figure 6-a). The flow rate (0.4 µL/min) and OTA-BSA concentration (50 µg/mL) used were the same as previously optimized for the detection module. The same applies for the subsequent washing (4 µL/min) and secondary antibody flow steps (0.4 µL/min). After the first washing step, the closed adapters were changed to the positions highlighted in Figure 6-b). Here, the closed adapters were carefully pushed down until contact with the bottom PDMS membrane was made. This provides a higher air pressure in the IC to prevent unintended contamination with anti-OTA IgG or SRP solutions prior to the stabilization of the APTE interface. A solution of red or white wine containing 12.5% NaH_2PO_4/K_2HPO_4 at pH 7 (non-contaminated or spiked with OTA) was then introduced through the top left inlet. A PRP prepared with 18.5% PEG and 4.5% NaH_2PO_4/K_2HPO_4 in ultrapure water and at pH 7 was inserted through the top right inlet. A solution of 3.75 µg/mL anti-OTA IgG in PBS was flowed through the center inlet. The flow rates used were 1 µL/min, 0.2 µL/min and 0.25 µL/min, respectively. After the stabilization of all 3 flows, which occurred after 5 to 10 min, the closed adapter of the IC are removed, as shown in Figure 6-c), allowing the liquid to flow inside. The flow stability was monitored using a Model #MD600 inverted microscope from AmScope, equipped with a digital camera. After 15 minutes of continuous flow, the transition from the conditions in Figure 6-c) to 6-d) was performed by first stopping the flow of SRW and anti-OTA IgG solutions, leaving the PRP flowing only, at 0.5 µL/min for about 1 min. Then, plain PBS

solution was introduced through the detection chamber at 4 µL/min for washing. While the detection chamber was being washed, all the required closed adapters and outlet tubing shown in Figure 6-d) were placed in their positions. Then, secondary antibody is flowed and the fluorescence quantification is performed under the microscope as previously described in the methods section for the straight channel icFLISA.

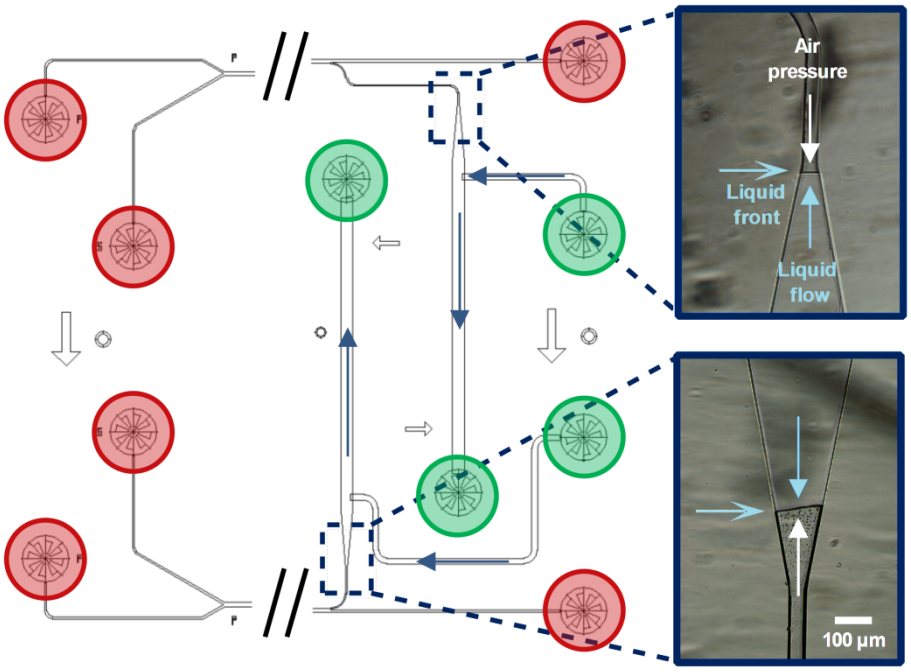

Figure S13 Schematics and bright field images of the method used to control the liquid flow using closed adapters, identified as red circles. Green circles identify inlets and outlets with open adapters. The blue arrows identify the liquid flow. The bright field microscopy images were acquired with the liquid flowing as indicated by the arrows.

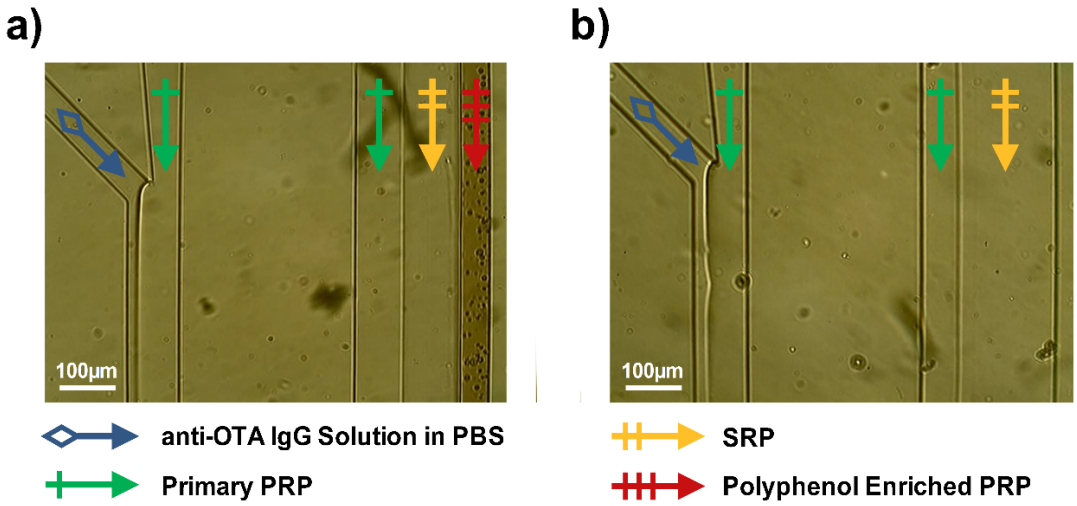

Figure S14 Bright field microscopy images of the control points for monitoring both interface position and IgG solution flow stability, during the integrated ATPE-icFLISA experiments. Images a) and b) were captured during red and white wine processing, respectively.